Progress In Electromagnetics Research C, Vol. 79, 199–208, 2017

Development of an Improved Response Ultra-Wideband Antenna Based on Conductive Adhesive of Carbon Composite

Erick Reyes-Vera*, Mauricio Arias-Correa, Andrés Giraldo-Muñoz, Daniel Cataño-Ochoa, and Juan Santa-Marín

Abstract—Ultra-wideband (UWB) antennas have advantages such as high data rates, improved multipath resistance and low power consumption. In this work, UWB patch antennas based on electrically conductive adhesive were manufactured with a simple technique and evaluated in the laboratory. Results showed that the thickness of the samples ranged from 207 to 261 μm. The bandwidth optimization obtained was 200% compared to a traditional copper-layer antenna. UWB antennas showed an average bandwidth of 8.558 GHz in the region 609 MHz to 9.105 GHz. The antennas covered the whole of UHF band, L band, S band, C band and part of X band. Finally, the proposed technique allows reducing the size of patch by 70% for low frequencies of operation, while achieving a similar performance.

1. INTRODUCTION

Recently, interest in ultra-wideband (UWB) antennas has increased. Since in 2002 Federal Communications Commission (FCC) approved a frequency range from 3.1 GHz to 10.6 GHz for commercial applications, UWB antennas have become a very interesting alternative for new developments in both research and manufacturing communities [1]. Compared to traditional antennas, UWB antennas have advantages such as high data rates, improved multipath resistance and low power consumption [1]. These advantages make UWB antennas interesting devices for medical and biological applications, such as WBAN systems [2, 3]. Even more, such characteristics enable coexistence of UWB antennas and narrowband systems [3, 4].

Microstrip antennas are low-cost devices, easy to manufacture and easy to integrate with electronic circuits [5–9], but these antennas usually operate over a limited frequency range. Accordingly, recent research articles have been focused on developing techniques to increase bandwidth of microstrip antennas by implementing fractals design, using metamaterials or replacing copper layers by new composites [4, 10–14], while other authors focus on radiation problems using semi-analytical models [15–18]. Development of microstrip antennas based on metamaterials to improve parameters such as the gain and bandwidth of conventional antennas has been studied previously by other authors [4, 19–21]. A promising technique uses new materials, which have low cost, light weight, high thermal conductivity and corrosion resistant feature, to replace copper layers. New materials, designs and manufacturing techniques have been introduced. Recently, microstrip antennas based on graphene [12, 22, 23], graphite [24], carbon nanotubes [13, 25–27] and conductive polymers [28] are under development.

Composites modified with single-wall carbon nanotubes (CNT) have been used to develop a low-profile wideband microstrip-fed monopole antenna, which operates over 24 to 34 GHz range [26]. The authors found that antennas with CNT had low dispersion characteristics over the frequency range of operation, and the housing effect was smaller than the same antenna fabricated with copper layers. On the other hand, continuous carbon fiber composite (CCFC) material has been used by other

Received 18 September 2017, Accepted 3 November 2017, Scheduled 26 November 2017

* Corresponding author: Erick Reyes-Vera (erickreyes@itm.edu.co).

The authors are with the Faculty of Engineering, Instituto Tecnológico Metropolitano, Medellin, Colombia.

authors [29] to manufacture reconfigurable transmitter/receiver communication systems. Probe-fed rectangular microstrip-patch antennas were manufactured, and the authors demonstrated that frequency of operation of a probe-fed patch antenna could be reconfigured by rotating the patch around the probe, operating over an anisotropic ground plane made of RCCFC composite, which allowed radiating modes with a current distribution component parallel to the fiber, acting as a mode filter.

Another UWB antenna was developed using Kapton as substrate and polyamide for the patch layer [30]. The measurements showed an improved performance of this antenna with frequency ranging from 2.2 to 14.3 GHz. This range covers industrial, scientific and medical (ISM) bands and the standard 3.1–10.6 GHz. Antennas with graphene nanoflakes have also been printed with an operating range from 984 to 1052 MHz [23]. In that study, the authors observed that the material was stable when thermal or electrical changes were applied. The screen printing manufacturing technique was used because of its low cost. The implementation of this new alternative composite is very interesting because copper is conductive, but its conductivity is fixed. Then, to change the frequency response of a copper antenna, a change in the geometry or dimensions is necessary. On the other hand, antennas based on composite material have an additional degree of freedom, the conductivity tensor of the composite. In that sense, to change the frequency response of a composite antenna, it may be sufficient to change the volume fraction of carbon particles into the mixture or its thickness as shown by Brosseau et al. [31]. The addition of carbon particles to an insulating polymer modifies the permittivity and conductivity of the material. Moreover, several reports studied the electrical behavior of these composites (carbon-polymer mixtures) and demonstrated that it presents a particular response. Since they have an insulator-conductor transaction, which depends on carbon concentration [13, 31–34], the antenna performance can be improved without changing the patch geometry or its dimensions when using composite antennas [26, 35].

Unlike the screen printing technique, the manufacturing processes mentioned above are expensive. When antennas are manufactured using graphene or carbon nanotubes, costs are very high, mainly because of materials costs. Furthermore, specialized equipment is required to obtain layers with high quality onto dielectric substrates during the antennas fabrication.

There are other processes described in the literature used to obtain conductive patch antennas. The article described in [36] developed an approach to decrease the silver content for filling conductive adhesives with silver particles (about 70–90 weight percent). This approach was developed, since the use of high silver contents generate a high-cost process. The authors used weak interactions (electrostatic, ionic or hydrogen bonding) between surface-modified nano-sized silver particles so that the particles undergo a self-structuring/orientation process in the liquid adhesive film (fixed through the curing process). The experimental validation of the system showed the successful replacement of the original organic coating by the silver particles. However, it was not possible to disperse the silver particles in the resin to nano-size, so that the distribution in the cured film is in principle as simulated but not as proper as expected. Besides, the approach was not successful at obtaining a conductive pathway to allow decreasing the amount of silver particles. On the other hand, electrically conductive adhesives (ECAs) exhibit many advantages such as printability and low-temperature processability. Printed antennas, which are based on the electrically conductive adhesives (ECAs), are a very promising alternative fabrication method of RFID tag antennas, due to both productivity and cost benefits. Other benefits of the method are that thinner shapes can be obtained, and the antennas are more environmentally friendly. In the work described in [37], the authors introduced silver microflake-filled ECAs as a candidate for the RFID tag antenna applications. ECAs have some advantages when they are compared to the conventional antenna preparation methods.

In this work, UWB patch antennas manufactured with a simple technique were evaluated in the laboratory. The manufacturing technique was used to obtain patch antennas based on electrically conductive adhesive applied on an FR4 substrate. The antennas (thickness and chemical composition) were characterized using a scanning electron microscope to evaluate the manufacturing process. Return losses and radiation patterns were measured, and the results were compared to those obtained for a traditional copper-layer patch antenna. The contribution of this work is related to several aspects: 1. Simple manufacturing process of the antenna 2. An ultra-wide band antenna is obtained by a simple design 3. Patch antennas can be miniaturized by the proposed technique.

2. METHODOLOGY

The preparation of electrically conductive adhesive based on composite material (polymer-carbon mixtures) plays an important role in this work because the material can be used to replace the copper layers. The polymer matrix selected in this investigation was EVA (Ethylene-Vinyl acetate), blended with an adhesive with a high carbon volume fraction and semiconductor particles. Since those materials can behave as insulators or conductive materials (as reported by Brosseau et al. [31]) depending on carbon concentration, it is important to optimize the quantity of carbon particles in the mixture and the manufacturing process. Therefore, the composite studied in this work has permittivity and conductivity simultaneously, and their values depend on the thickness of the layer, volume fraction of the particles and matrix (carbon particles, semiconductor particles and EVA), and shape of carbon clusters dispersed into the polymer [31, 34, 38]. Accordingly, two important topics are explored in this article: the manufacturing process of composite antennas and the study of the radiation properties of composite antennas, which differ significantly from that reported for the copper antennas due to the differences in permittivity and conductivity of the composite layers. Accordingly, the geometry was not optimized. A standard geometry was selected to perform the tests on the proposed materials.

Once the composite was prepared, the proposed antenna was manufactured on an FR4 substrate and electrically conductive adhesive layers in the patch and ground plane. The FR4 substrate having a dielectric constant of $\varepsilon_r = 4.4$, loss tangent of $\delta = 0.002$ and thickness of 1.6 mm. The antenna patch was connected to the microstrip line providing a characteristic impedance of 50 Ω. Conductive adhesive has a thickness of ≈ 0.3 mm in order to increase the effective conductivity. The adhesive structure of the antennas is shown in Figure 1. The layer of adhesive was also used as ground plane, and it was applied to the rear side of the substrate covering the total surface.

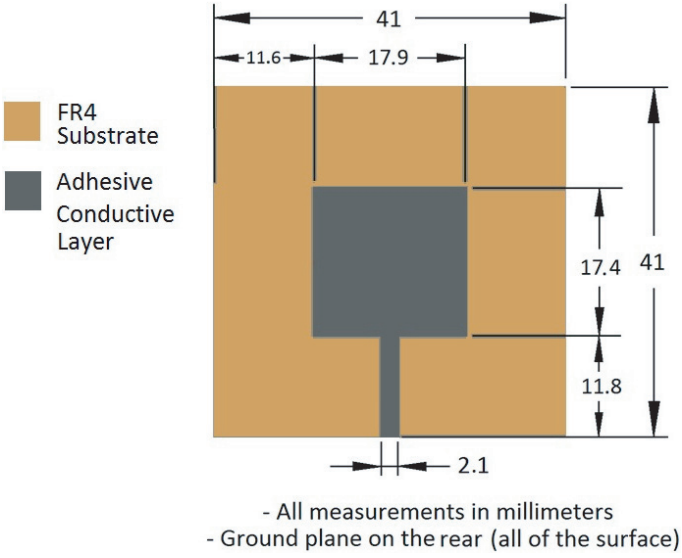

Figure 1. Geometry and dimensions of the designed electrically conductive adhesive patch antenna. Ground plane in the backside, covers the entire surface (41 mm × 41 mm).

Manufacturing of antennas was carried out in the polymers Laboratory of Instituto Tecnológico Metropolitano, using standard manufacturing conditions. The procedure was simplified to improve repeatability as described below, as illustrated in Figure 2. Initially, a sheet of FR4 without conductive layer, with dimensions of 41 mm × 41 mm, was cut using a CNC router. The sheet was used as a dielectric substrate of the antenna. Using a 3D printer, a 1.3 mm thick PLA mask was printed with the geometric dimensions of the patch ($W = 17.8$ mm, $L = 17.4$ mm). After that, the mask was pressed over the substrate, and a layer of conductive adhesive was applied onto the FR4. The pressure was applied to control thickness of the patch. The thickness of the mask was controlled to be around 0.3 mm (as seen in Figure 2).

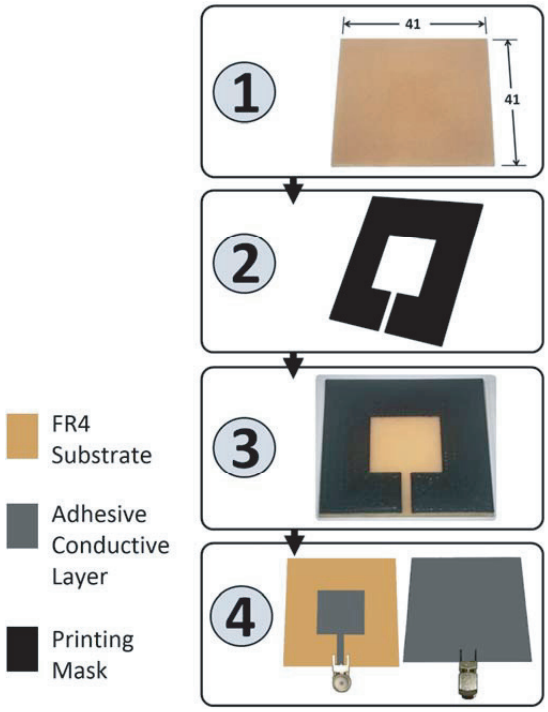

Figure 2. Summary of manufacturing procedure for electrically conductive adhesive antennas with FR4 substrate. 1. Substrate 2. Printed Mask 3. Mask superimposed during antennas fabrication 4. Conductive layer over FR4 substrate and rear of manufactured antenna

The rear surface of the FR4 substrate was applied with a conductive adhesive to create the ground plane of the antenna. PLA masks were removed, and a SMA connector (SMA-J-P-H-ST-TH1) was added to connect both the patch and ground plane through contact points.

After applying the layer, the antennas were dried during 24 hours to obtain the best conductivity value between patch and SMA connector. Subsequently, antennas were tested to validate the prototypes. Conductivity was the first parameter to measure, and after that, signal analysis was carried out. The signal analysis was taken as an evaluation parameter to determine if the prototype was rejected. In order to evaluate the quality and repetitivity of the manufacturing technique, four samples were manufactured, and all of them were tested. A summary of the manufacturing process is shown in Figure 2.

After applying the conductive adhesive, samples were cut to evaluate through observation of transverse section. Samples were mounted in a resin, and a metallographic polishing was done by emery papers up to 1000 grit size. After polishing, the samples were inspected in a JEOL 7100F Field Emission Scanning Electron Microscope (FE-SEM) with Energy Dispersive Spectrometry (EDS) to evaluate the structure within the layer. In all cases, at least 10 measurements of thickness were performed, and the average and standard deviation were reported.

3. EXPERIMENTAL RESULTS

Images of transverse section of one representative developed antenna and chemical compositions of sample are shown in Figure 3, Figure 4 and Figure 5.

The substrate, to which the conductive adhesive was applied, was reinforced with glass fibers in order to improve the capacitance and to improve mechanical resistance of the samples (Figure 3). The thickness of the samples is shown in Table 1.

From the results, it can be concluded that the thickness of the samples ranges from 207 to 261 µm. The manufacturing process used to obtain the antennas includes the polymerization of a resin used as a matrix to gather carbon and semiconductor particles. During the polymerization pores can be formed in

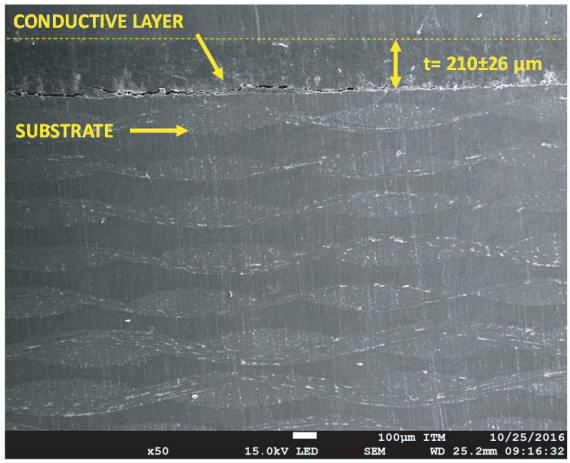

Figure 3. Image of substrate and conductive layer.

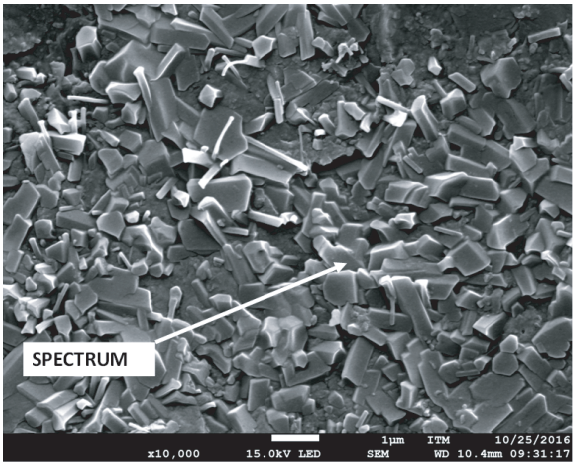

Figure 4. Detail of the particles (crystals) in conductive layer.

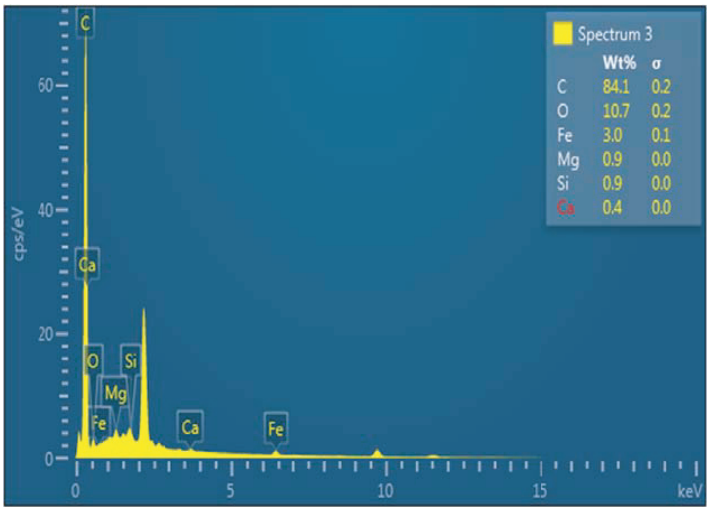

Figure 5. Spectrum showing the chemical composition of the electrically conductive layer.

Table 1. Average thickness and standard deviation of developed antennas.

Sample	Average thickness (µm)	Standard deviation	Error (%)
1	210	26	12
2	238	21	9
3	261	21	8
4	207	39	19

the layers since the application was done manually. Moreover, during the polishing procedure required to analyze the samples in the SEM (to obtain Figure 3), defects can be induced in the sample, and the layers can be detached from the substrate. On the other hand, the error in the thickness is caused by the manufacturing process (the differences in thickness are around 26%). Despite the defects and the differences in the thicknesses observed in the samples and shown in this manuscript, the replicas show that the antennas perform very similarly in terms of reflection coefficient. The optimization of

the manufacturing process to obtain small variation of the thickness is beyond the scope of this article. In addition, small differences in thickness could be induced by the contraction of the water-dissolved polymer during manufacturing of the antenna.

The structure of the antenna samples is composed of a high carbon matrix (conductive polymer) and conductive particles (crystals). The particles are complex iron oxides added to increased conductivity of the polymer. The microstructure of particles is shown in Figure 4.

An energy dispersive spectrum showing the chemical composition of the sample is shown in Figure 5. The determination of the elements in the layers was done by using and Energy Dispersive Spectrometry (EDS). In that technique, electrons are delivered to the sample, and they generate characteristics X-rays. After that, the X-rays generated in the sample are collected and classified to evaluate the amount of certain element in the sample depending on the counts of X-rays received in the detector. The vertical axis is the number of counts per second (count per second, cps), and it is related to number of X-ray photons received in the detector which is proportional to the concentration of the element in the sample. The x axis shows the energy of the characteristics X-rays received in the detector. From that spectrum it can be concluded that particles comprise iron, magnesium, silicon and calcium. Since the oxygen contents are high, the crystals are complex oxides used to provide electrical conductivity to the polymer.

Electrical characterization of the proposed antennas was done using a ZVA24 Rohde & Schwarz Vector Network Analyzer. Figure 6 shows a comparison between the reflection coefficients obtained by the proposed antenna and the same antenna using copper layers. For the antenna with copper layers, the operating frequency can be calculated using conventional theory. It presents a main resonant frequency at 4 GHz. However, this design shows strong reflection at 4 GHz because the system has a poor impedance matching between the microstrip line and the patch. On the other hand, the proposed antenna based on composite materials shows an excellent impedance mismatch in an ultra-wide band (From GHz to GHz). In this case, the optimal operating frequency is close to 6 GHz because the reflection coefficient reached -36 dB approximately. The main difference between the two antennas is that conductive layer of the proposed antenna has conductivity and permittivity simultaneously. As explained before, it is caused by the presence of a polymer matrix and the carbon and semiconductor particles. Then, it is similar to have double substrate layers (FR4 and polymer materials) between the patch and the ground, which help impedance matching and increase the bandwidth of our antenna. On the other hand, the presence of some peaks after 10 GHz could be related with dispersive characteristics of FR4 material. However, as shown in Figure 6, the composite material helps to mitigate these effects. It is because the polymer modifies the effective permittivity of the system, and it can even induce displacements in resonance frequencies. This physical principle is used in other applications such as

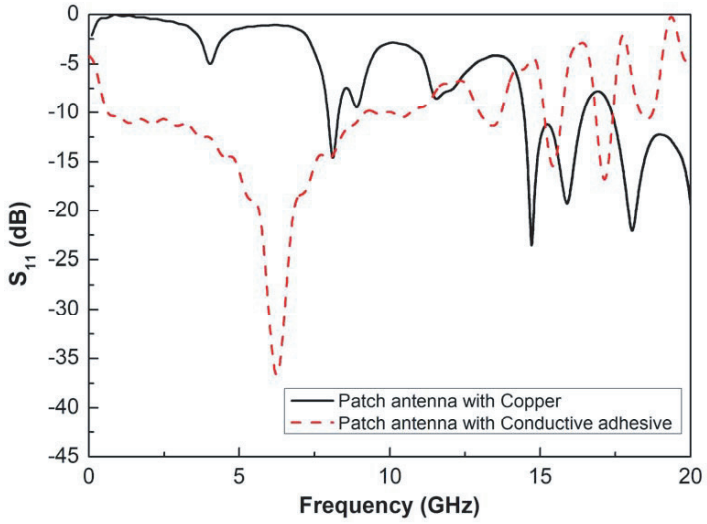

Figure 6. Comparison of S_{11} measurements between fabricated copper and electrically conductive adhesive antennas.

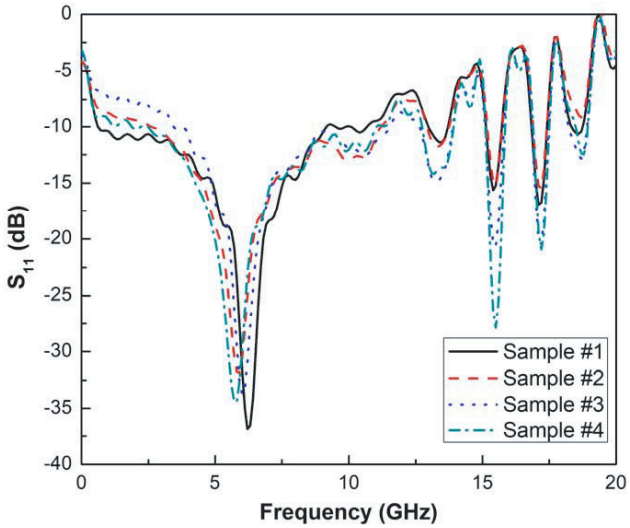

Figure 7. Measured S_{11} parameter of proposed antenna for different samples.

Table 2. Parameters obtained during reflection coefficient analysis.

Parameter	sample #1	sample #2	sample #3	sample #4	Mean	Standard Deviation
f_{r1} (GHz)	6.2440	5.8596	6.0252	5.7494	5.9424	0.2152
Δf_1 (GHz)	8.5315	8.6451	8.1211	8.5851	8.5583	0.2377
f_{r2} (GHz)	13.3490	13.3310	13.2940	13.3256	13.3283	0.0229
Δf_2 (GHz)	0.8322	0.8322	1.2617	1.1669	0.9996	0.2579
f_{r3} (GHz)	15.4290	15.4680	15.4598	15.4880	15.4639	0.0245
Δf_3 (GHz)	0.5874	0.5649	0.7104	0.7322	0.6489	0.0847
f_{r4} (GHz)	17.1390	17.1590	17.1711	17.2043	17.1651	0.0269
Δf_4 (GHz)	0.5906	0.5202	0.6416	0.6027	0.5967	0.0506
f_{r5} (GHz)	18.5280	18.5640	18.5643	18.6966	18.5642	0.0742
Δf_5 (GHz)	0.3926	-	0.6981	0.4478	0.4478	0.1628

sensors to measure concentration changes in liquids or solids [21, 39]. Figure 7 shows the reflection coefficient by four manufactured samples. From the figure, it can be concluded that all developed samples showed a very similar behavior. The same frequency peaks and bandwidth were observed in the four samples.

Another important aspect is the UWB behavior observed for the developed antennas. In the region of 609 MHz to 9.105 GHz (more than 200% of fractional bandwidth), the proposed antenna covered a major part (80%) of the UWB spectrum for commercial applications. The antennas covered the whole of UHF band, L band, S band, C band, and part of X band. In addition, the characterized samples presented four peaks found in 13.328 GHz, 15.464 GHz, 17.165 GHz and 18.564 GHz as summarized in Table 2. Table 2 shows a detailed analysis of different samples (resonant frequencies and bandwidth for each resonant peak). The results obtained in this work showed that all manufactured antennas were very similar since the fluctuations of the resonance frequency and bandwidth are smaller than 260 MHz, which can be associated with fluctuations in the thickness of the conductive adhesive layer.

On the other hand, the implementation of the conductive adhesive allows miniaturizing the dimension of the antenna, especially at lower frequencies. For example, an antenna whose operating frequency is 700 MHz, and the dimensions will be around 130 mm × 80 mm (10400 mm^2). If dimensions were compared to the antenna described in this article, they would be 17 mm × 17 mm (289 mm^2). Accordingly, the area of the device would be 36 times smaller than copper layer patch antennas. Then,

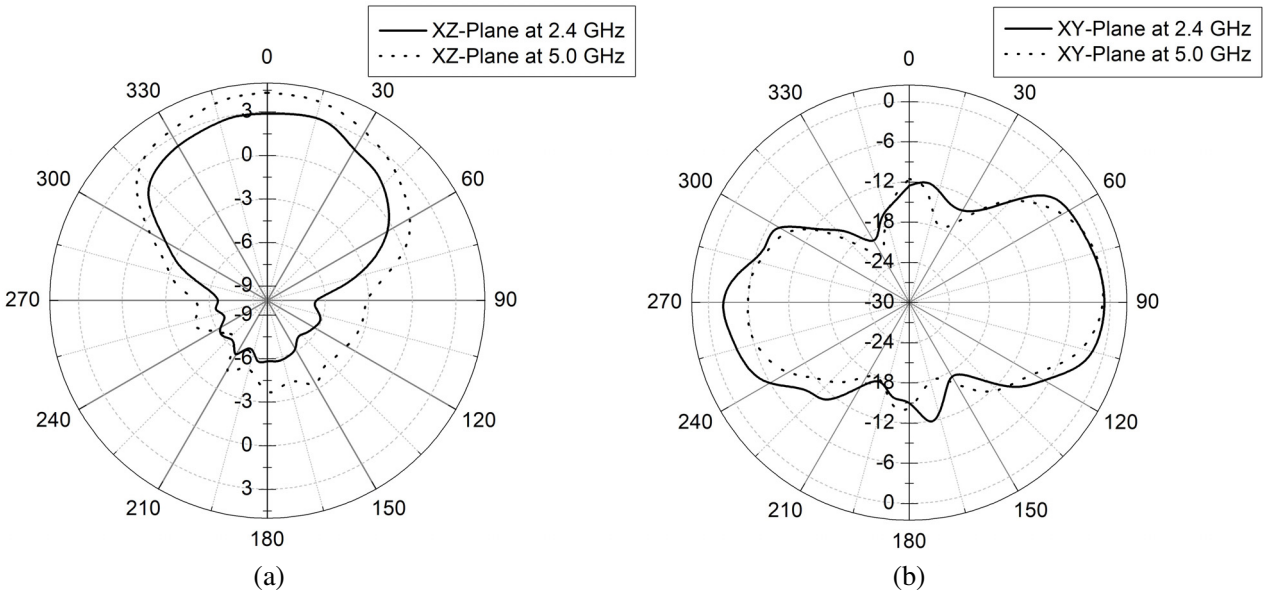

Figure 8. Radiation patterns at 2.4 GHz and 5 GHz. (a) XZ-plane; (b) XY-plane.

it is possible to conclude that developed antennas allow us to miniaturize the patch antenna whose operating frequency is less than 2.4 GHz, reducing its dimensions by up to 70%. This estimation was made following the procedure explained in [40].

Finally, Figure 8 presents the measured radiation patterns in two principal planes at 2.4 GHz and 5 GHz (it must be pointed out that due to equipment limitations, radiation patterns were obtained only in these frequency values). From these results, it can be concluded that the constructed antennas have an omnidirectional behavior. In the case of XZ-plane, the radiation of antenna is sent mainly in one direction with a half-power beamwidth $\approx 138°$. This shows that the antenna radiates in all directions and could even cover a wider area. This result is important since it implies that antennas are suitable for wireless communication such as Wi-Fi, Bluetooth, and WiMAX/WLAN applications. A symmetrical radiation pattern was observed for both analyzed frequencies.

4. CONCLUSION

In this work, Ultra-Wide Band (UWB) patch antennas using an electrically conductive adhesive were manufactured with a simple technique, and their behavior was evaluated in the laboratory.

The results showed that the thickness of the carbon composite samples was from 207 to 261 µm. Electrical characterization of proposed antennas shows that the manufacturing process provided high repeatability and thickness control. In addition, fabricated antennas show low dispersion characteristics over the frequency range of interest and so may be used in wireless applications

Experimental results show that carbon composite antenna has good performance from 609 MHz to 9.105 GHz and an average bandwidth of 8.558 GHz. The bandwidth optimization obtained was 200% higher compared to copper traditional antennas.

Finally, the proposed antennas covered the whole UHF band, L band, S band, C band, and part of X band. The manufacturing technique allows optimizing the geometry of antennas since it is possible to miniaturize the geometry to obtain the same electrical resonance.

ACKNOWLEDGMENT

The authors would like to thank the support given under the project P15106 funded by Instituto Tecnológico Metropolitano. In addition, authors thank to the Universidad Javeriana of Bogotá by let us use the ZVA24 Rhode & Schwarz Vector Network Analyzer to make the experimental measurements.

REFERENCES

1. Tariqul, M. and R. Azim, "Recent trends in printed Ultra-Wideband (UWB) antennas," *Advancement in Microstrip Antennas with Recent Applications*, InTech, 2013.
2. Chi, Y. J. and F. C. Chen, "On-body adhesive-bandage-like antenna for wireless medical telemetry service," *IEEE Trans. Antennas Propag.*, Vol. 62, No. 5, 2472–2480, 2014.
3. Ho, C. K., T. S. P. See, and M. R. Yuce, "An ultra-wideband wireless body area network: Evaluation in static and dynamic channel conditions," *Sensors Actuators A Phys.*, Vol. 180, 137–147, Jun. 2012.
4. Islam, M. T., M. Samsuzzaman, M. R. I. Faruque, and M. M. Islam, "Compact metamaterial antenna for UWB applications," *Electron. Lett.*, Vol. 51, No. 16, 1222–1224, 2015.
5. Ferreira, D. B., C. B. de Paula, and D. C. Nascimento, "Design techniques for conformal microstrip antennas and their arrays," *Advancement in Microstrip Antennas with Recent Applications*, InTech, 2013.
6. Thi, T. N., S. Trinh-Van, G. Kwon, and K. C. Hwang, "Single-feed triple-band circularly polarized spidron fractal slot antenna," *Progress In Electromagnetics Research*, Vol. 143, 207–221, 2013.
7. H. W. Lai, K. M. Mak, and K. F. Chan, "Novel aperture-coupled microstrip-line feed for circularly polarized patch antenna," *Progress In Electromagnetics Research*, Vol. 144, 1–9, 2014.
8. Chen, L., X.-S. Ren, Y.-Z. Yin, and Z. Wang, "Broadband CPW-fed circularly polarized antenna with an irregular slot for 2.45 GHz RFID reader," *Progress In Electromagnetics Research Letters*, Vol. 41, 77–86, 2013.
9. Zuo, S., Q.-Q. Liu, and Z.-Y. Zhang, "Wideband dual-polarized crossed-dipole antenna with parasitical crossed-strip for base station applications," *Progress In Electromagnetics Research C*, Vol. 48, 159–166, 2014.
10. Singh, H. S., G. K. Pandey, M. K. Meshram, and P. K. Bharti, "Metamaterial-based UWB antenna," *Electron. Lett.*, Vol. 50, No. 18, 1266–1268, 2014.
11. Dai, Y., B. Yuan, G. Luo, and X. Zhang, "Ultra-wideband patch antenna with metamaterial structures," *2015 IEEE 16th International Conference on Communication Technology (ICCT)*, No. c, 403–404, 2015.
12. Perruisseau-Carrier, J., "Graphene for antenna applications: Opportunities and challenges from microwaves to THz," *2012 Loughbrgh. Antennas Propag. Conf.*, 1–4, Nov. 2012.
13. Mehdipour, A., A. R. Sebak, C. W. Trueman, I. D. Rosca, and S. V. Hoa, "Advanced conductive carbon fiber composite materials for antenna and microwave applications," *2012 IEEE Antennas Propag. Soc. Int. Symp. (APSURSI)*, Vol. 1, No. c, 1–2, 2012.
14. Zhu, F., et al., "Ultra-wideband dual-polarized patch antenna with four capacitively coupled feeds," *IEEE Trans. Antennas Propag.*, Vol. 62, No. 5, 2440–2449, 2014.
15. Valagiannopoulos, C. A., "On examining the influence of a thin dielectric strip posed across the diameter of a penetrable radiating cylinder," *Progress In Electromagnetics Research C*, Vol. 3, 203–214, 2008.
16. Valagiannopoulos, C. A., "Single-series solution to the radiation of loop antenna in the presence of a conducting sphere," *Progress In Electromagnetics Research*, Vol. 71, 277–294, 2007.
17. Valagiannopoulos, C. A., "High selectivity and controllability of a parallel-plate component with a filled rectangular ridge," *Progress In Electromagnetics Research*, Vol. 119, 497–511, 2011.
18. Valagiannopoulos, C. A., "A novel methodology for estimating the permittivity of a specimen rod at low radio frequencies," *Journal of Electromagnetic Waves & Applications*, Vol. 24, Nos. 5–6, 631–640, 2010.
19. Catano-Ochoa, D., D. E. Senior, F. Lopez, and E. Reyes-Vera, "Performance analysis of a microstrip patch antenna loaded with an array of metamaterial resonators," *2016 IEEE International Symposium on Antennas and Propagation (APSURSI)*, 281–282, 2016.
20. Castellanos, L. M., F. Lopez, and E. Reyes-Vera, "Metamateriales: Principales características y aplicaciones," *Rev. la Acad. Colomb. Ciencias Exactas, Físicas y Nat.*, Vol. 40, No. 156, 395, Oct. 2016.

21. Acevedo-Osorio, G., H. Muñoz Ossa, and E. Reyes-Vera, "Performance analysis of monopole excited split ring resonator for permittivity characterization," *2017 42nd International Conference on Infrared, Millimeter, and Terahertz Waves (IRMMW-THz)*, 1–2, 2017.
22. Hotopan, G. R., S. Ver-Hoeye, C. Vazquez-Antuna, A. Hadarig, R. Camblor-Diaz, M. Fernandez-Garcia, and F. Las Heras Andres, "Millimeter wave subharmonic mixer implementation using graphene film coating," *Progress In Electromagnetics Research*, Vol. 140, 781–794, 2013.
23. Leng, T., X. Huang, K. Chang, J. Chen, M. A. Abdalla, and Z. Hu, "Graphene nanoflakes printed flexible meandered-line dipole antenna on paper substrate for low-cost RFID and sensing applications," *IEEE Antennas Wirel. Propag. Lett.*, Vol. 15, 1565–1568, 2016.
24. Tadakaluru, S., W. Thongsuwan, and P. Singjai, "Stretchable and flexible high-strain sensors made using carbon nanotubes and graphite films on natural rubber," *Sensors (Basel)*, Vol. 14, No. 1, 868–76, Jan. 2014.
25. Trueman, C. W., A. Sebak, T. A. Denidni, S. V Hoa, A. Mehdipour, and I. D. Rosca, "Mechanically reconfigurable antennas using an anisotropic carbon-fibre composite ground," *IET Microwaves, Antennas Propag.*, Vol. 7, No. 13, 1055–1063, Oct. 2013.
26. Mehdipour, A., I. D. Rosca, A. R. Sebak, C. W. Trueman, and S. V. Hoa, "Carbon nanotube composites for wideband millimeter-wave antenna applications," *IEEE Trans. Antennas Propag.*, Vol. 59, No. 10, 3572–3578, 2011.
27. De Assis, R. R. and I. Bianchi, "Analysis of microstrip antennas on carbon fiber composite material," *J. Microwaves, Optoelectron. Electromagn. Appl.*, Vol. 11, No. 1, 154–161, Jun. 2012.
28. Rmili, H., J.-L. Miane, H. Zangar, and T. Olinga, "Design of microstrip-fed proximity-coupled conducting-polymer patch antenna," *Microw. Opt. Technol. Lett.*, Vol. 48, No. 4, 655–660, Apr. 2006.
29. Mehdipour, A., T. A. Denidni, A. Sebak, and C. W. Trueman, "Reconfigurable TX/RX antenna systems loaded by anisotropic conductive carbon-fiber composite materials," *IEEE Trans. Antennas Propag.*, Vol. 62, No. 2, 1002–1006, Feb. 2014.
30. Khaleel, H. R., H. M. Al-Rizzo, D. G. Rucker, and S. Mohan, "A compact polyimide-based UWB antenna for flexible electronics," *IEEE Antennas Wirel. Propag. Lett.*, Vol. 11, 564–567, 2012.
31. Brosseau, C., et al., "Dielectric and microstructure properties of polymer carbon black composites," *J. Appl. Phys.*, Vol. 81, No. 2, 882–891, Jan. 1997.
32. Song, T. Q., Y. Zhou, and L. X. Ma, "Study on relationship between carbon black and dielectric properties of tire rubber in UHF band," *Appl. Mech. Mater.*, Vol. 536–537, 1456–1459, 2014.
33. Bao, Y., et al., "Preparation and properties of carbon black/polymer composites with segregated and double-percolated network structures," *J. Mater. Sci.*, Vol. 48, No. 14, 4892–4898, Jul. 2013.
34. Lawandy, S. N., S. F. Halim, and N. A. Darwish, "Structure aggregation of carbon black in ethylene-propylene diene polymer," *Express Polym. Lett.*, Vol. 3, No. 3, 152–158, 2009.
35. Mehdipour, A., I. D. Rosca, C. W. Trueman, A. R. Sebak, and S. Van Hoa, "Multiwall carbon nanotube-epoxy composites with high shielding effectiveness for aeronautic applications," *IEEE Trans. Electromagn. Compat.*, Vol. 54, No. 1, 28–36, 2012.
36. Kowalik, T., M. Amkreutz, C. Harves, A. Hartwig, and S. J. Aßhoff, "Conductive adhesives with self-organized silver particles," *IOP Conf. Ser. Mater. Sci. Eng.*, Vol. 40, 12033, Sep. 2012.
37. Li, M. and C. Yang, "Conductive adhesives as the ultralow cost RFID tag antenna material," *Current Trends and Challenges in RFID*, InTech, 2011.
38. Zois, H., L. Apekis, and M. Omastová, "Electrical properties of carbon black-filled polymer composites," *Macromol. Symp.*, Vol. 170, No. 1, 249–256, Jun. 2001.
39. Lobato-Morales, H., A. Corona-Chavez, J. L. Olvera-Cervantes, R. A. Chavez-Perez, and J. L. Medina-Monroy, "Wireless sensing of complex dielectric permittivity of liquids based on the RFID," *IEEE Trans. Microw. Theory Tech.*, Vol. 62, No. 9, 2160–2167, Sep. 2014.
40. Saini, A., A. Thakur, and P. Thakur, "Effective permeability and miniaturization estimation of ferrite-loaded microstrip patch antenna," *J. Electron. Mater.*, Vol. 45, No. 8, 4162–4170, Aug. 2016.